Superconducting diamagnetic fluctuations in Sm-based underdoped cuprates studied via SQUID magnetometry

E. Bernardi,[1] A. Lascialfari,[1,2,3] A. Rigamonti,[1] L. Romanò,[4] M. Scavini,[5] and C. Oliva[5]
[1]*Department of Physics "A. Volta" and Unità CNISM-CNR, University of Pavia, Via Bassi 6, I-27100 Pavia, Italy*
[2]*Department of Molecular Sciences Applied to Biosystems, Universitá degli studi di Milano, Via Trentacoste 2, I-20134 Milano, Italy*
[3]*S3-CNR-INFM, I-41100 Modena, Italy*
[4]*Department of Physics and Unità CNISM-CNR, University of Parma, Parco Area delle Scienze 7A, I-43100 Parma, Italy*
[5]*Department of Chemistry and Electrochemistry, Universitá degli studi di Milano, I-20133 Milano, Italy*
(Received 27 April 2009; revised manuscript received 16 July 2009; published 3 February 2010)

High-resolution superconducting quantum interference device isothermal magnetization measurements in Al-doped Sm-based superconducting cuprates are presented, at the aim to analyze the properties of the underdoped, pseudogapped phase in regards of the superconducting fluctuations (SF) above T_c. In the optimally doped compound, the SF are well described by the conventional Ginzburg-Landau (GL) free-energy functional for three-dimensional anisotropic systems. On the contrary, in the underdoped compounds, obtained by Al for in-chain Cu substitution at constant oxygen content, dramatic differences are detected. The isothermal curves M_{dia} above T_c show an upturn field H_{up}, where $|M_{dia}|$ starts to decrease on increasing field. H_{up} is found to increase on increasing temperature. The experimental data on the field dependence of the diamagnetic magnetization above T_c can be justified by transforming the GL-Lawrence-Doniach functional into the one for a layered system of vortices with frozen amplitude of the order parameter but with strong phase fluctuations. It is argued that this behavior is characteristic of the underdoped phase of the cuprates, thus providing insights on the pseudogapped phase as accompanied by fluctuations in the phase of order parameter.

DOI: 10.1103/PhysRevB.81.064502 PACS number(s): 74.40.−n, 74.20.De, 74.72.−h

I. INTRODUCTION

On approaching the transition temperature T_c from above superconducting fluctuations (SF) occur, with an average order parameter $[\langle|\psi^2|\rangle]^{1/2}$ different from zero, as related to local concentration of fluctuating Cooper pairs.[1] As a consequence of SF, above T_c one can detect a Langevin-type diamagnetic magnetization $-M_{dia}(H,T)$, existing side by side with the paramagnetic contribution from fermionic carriers.[2] This *fluctuating diamagnetism* (FD) is enhanced in cuprate superconductors because of their small coherence length $\xi(T)$, reduced carrier density, strong anisotropy and high T_c. Since the size of the fluctuating pairs, on the order of $\xi(T)$, grows when the transition temperature is approached, $|-M_{dia}|$ is expected to exhibit a progressive increase on cooling from above. On the other hand, very high magnetic field H, comparable to the critical field $H_{c2}(0)$ must evidently suppress the SF's. Therefore, when $-M_{dia}$ at a given temperature is reported as a function of the field, an upturn in the field dependence is expected to occur. In the framework of the Ginzburg-Landau (GL) scenario this upturn is quantitatively described by means of an elaborated microscopic theory accounting for the short wavelength fluctuations and nonlocality.[1–3]

An introductory qualitative description of the field dependence of $-M_{dia}(H,T=\text{const})$ with an approximate estimate of the upturn field H_{up}, where $|M_{dia}|$ initiates to decrease, can easily be obtained from the GL free-energy functional in the assumption that the large part of the diamagnetic effects are due to superconducting granules with size on the order of $\xi(T)$ and then crudely applying the zero-dimensional condition. Then,[4,5] at the first-order fluctuation correction (Gaussian approximation), with the exclusion of the narrow critical region very close to T_c one can write

$$M_{dia} \approx -k_B TH[4\pi^2\xi_0^2\xi^2(T)/5\Phi_0^2]/[\varepsilon + 2\pi^2\xi_0^2\xi^2(T)H^2/5\Phi_0^2] \quad (1)$$

with $\varepsilon=[T-T_c]/T_c$, so that the upturn in the field dependence of M_{dia} is estimated to occur around $H_{up} \approx \varepsilon\Phi_0/4\xi_0^2$.

While in BCS superconductors the values of H_{up} are rather small,[2,5] typically around 50–100 Oe, in cuprate superconductors, because of the small coherence length, the upturn field is expected at very high values of H. Typically, for ε around 10^{-2}, H_{up} could be in the range above 10 T. The fact that quenching of the Cooper pairs is expected only at very high field, explains why from the GL functional for layered superconductors, in the Lawrence-Doniach (LD) form[1,2,6]

$$F_{LD}[\psi] = \sum_l \int d^2r \left(\alpha|\psi_l|^2 + \frac{\beta}{2}|\psi_l|^4 + \frac{\hbar^2}{4\pi^2 m}\left|\left(\nabla_{\parallel} - \frac{2ie}{c\hbar}A_{\parallel}\right)\psi_l\right|^2 + \Im|\psi_{l+1}-\psi_l|^2 \right) \quad (2)$$

(where ψ_l is the order parameter of the lth plane and the phenomenological constant $\Im$ is related to the Josephson coupling between adjacent planes) the isothermal magnetization curves are rather well justified in optimally doped superconducting cuprate, as it is pointed out by measurements in $YBa_2Cu_3O_7$ (YBCO).[7–9]

On the other hand, it is well known that underdoped cuprates are characterized by the occurrence of a pseudogapped phase (PG) below a doping-dependent temperature $T^* \gg T_c$. Although in general terms the PG opening is essentially a transfer of spectral weight from the low-energy to the high-energy range, the real nature of the underdoped phase in cuprates and the underlying physical mechanism are still elusive, in spite of the large number of experimental and theoretical efforts.[10,11] One of the main line of the speculative analyses of the PG phase involves the possible occurrence of fluctuations of various character.[10]

In YBCO-type cuprates the underdoped phase is usually obtained by controlling the oxygen content. However, the investigation of this region is rather difficult because of the structural changes accompanying the increase in δ. In fact, oxidation triggers a progressive short-range ordering of Cu1-O4 ions along the crystallographic b direction, which in turn promotes a variety of long-range oxygen orderings and phase transitions.[12] Recent diffuse scattering studies have probed the nature and the spatial (nanodistributions) distributions of oxygen superstructures in pure[13,14] and Ca-doped[14] YBCO as a function of δ. Moreover, it is quite difficult to control the chain length for the intermediate oxygen concentrations, since, for each δ value, the oxygen distribution within the xy, $z=0$ plane is a function of the annealing conditions (T and pO_2) and can also vary as a consequence of ageing.[12]

In this paper, the underdoped phase has been obtained by doping with Al the YBCO-parent-compound $SmBa_2Cu_3O_7$, thus obtaining the underdoped system $SmBa_2Cu_{2.85}Al_{0.15}O_7$ where the oxygen concentration in the chains' plane is not touched to a good extent.[15] To this purpose, aluminum can be considered a suitable dopant since: (i) it is a nonmagnetic ion; (ii) it substitutes for copper only on one of the two crystallographic nonequivalent positions, Cu1 (0,0,0);[16] (iii) throughout suitable annealing routes[17,18] it is possible to control the aluminum distribution and, as a consequence, the mean length of the Cu-O chain fragments in fully oxidized samples (see Fig. 10 of Ref. 17). For what concern this last point, in a previous paper we have shown that the increase in the main length of the chain fragments in $SmBa_2Cu_{2.85}Al_{0.15}O_{6+\delta}$,[18] at fixed Al and oxygen concentration, induced a pronounced enhancement of the superconducting properties (i.e., of T_c and Meissner fraction).[18]

Here we report high-resolution superconducting quantum interference device (SQUID) isothermal magnetization measurements in that family of Sm-based superconducting cuprates, for both optimally doped and underdoped systems. The primary aim of our work is to analyze the properties of the underdoped, pseudogapped phase in regards of the SF above T_c.

It will be shown that for the optimally doped compound having $T_c(H \cong 0)=94.5$ K, the SF are well described by the conventional GL free-energy functional for three-dimensional anisotropic systems.[19] For that compound, in fact, the diamagnetic magnetization curves M_{dia} as a function of temperature for various H cross each other at $T_c(H=0)$ when the data are scaled by the square root of the magnetic field H, while the isothermal magnetization curves $M_{dia}(T=\text{const},H)$ do not exhibit any upturn field up to 7 T.

At variance in the underdoped compound, relevant differences are detected and the SF exhibit unconventional GL character: the isothermal curves M_{dia} above T_c show an upturn field H_{up}, where $|M_{dia}|$ starts to decrease on increasing field and M_{dia} measured as a function of temperature at different fields H do not scale at $T_c(0)$ as the square root of the magnetic field. Very interestingly, H_{up} is found to increase on increasing temperature. This behavior, obtained here with neat clarity in underdoped high-temperature superconductors, rules out the possibility of ascribing this phenomenon to local inhomogeneities yielding a diffuse transition.

II. EXPERIMENTALS

Polycrystalline samples of $SmBa_2Cu_{3-y}Al_yO_{6+\delta}$ were synthesized by solid-state reaction starting from BaO_2 (Aldrich 95%), Sm_2O_3, CuO, and Al_2O_3 (all Aldrich 99.99%). Powders were mixed, pressed into pellets, and allowed to react in pure oxygen at 960 °C for a total time of 96 h with one intermediate cooling, grinding, and repelletization step. Samples were subsequently annealed for 96 h at $T=400$ °C and $P(O_2)=1$ atm to induce oxidation. Following the annealing procedure suggested by Ref. 22, an aliquot of $y=0.15$ sample was annealed at $T=800$ °C and $P(O_2)=10^{-4}$ atm for 96 h and then at $T=400$ °C and $P(O_2)=1$ atm for the same time to reoxidize the sample. The annealing time have been chosen in order to avoid gradients of oxygen activity within the sample (see Ref. 15 for a discussion of the oxygen diffusion coefficient as a function of T and pO_2). This procedure induces "clustering," i.e., a nonstatistical distribution of Al ions within the xy, $z=0$ plane. In this way longer Cu1-O4 chains (~20 Å long[18]) in respect to a nonclustered sample, taking fixed Al and O4 concentrations, have been obtained.

The δ values for each sample has been determined by means of thermogravimetric analysis using the method described in Ref. 15: $\delta=0.98(1)$ for the Al-free sample and $\delta=0.96(1)$ for the $y=0.15$ "clustered" one.

The structure of the samples has been determined by means of x-ray powder diffraction patterns, collected at the high-resolution powder x-ray diffractometer at beam line ID31 at ESRF, Grenoble, France[20] using a wavelength of $\lambda=0.33483(1)$ Å. Diffracted intensities were detected through nine Si(111) analyzer crystals. Rietveld refinements have been performed using the GSAS software suite[21] and its graphical interface EXPGUI.[22]

The $SmBa_2Cu_3O_{\approx 7}$ sample was single-phase orthorhombic [*Pmmm* space group, $a=3.83819(1)$ Å, $b=3.90042(1)$ Å, and $c=11.70636(4)$ Å at 80 K] while the clustered $SmBa_2Cu_{2.85}Al_{0.15}O_{\approx 7}$ one showed both a tetragonal phase [space group $P4/mmm$, $a=3.89098(3)$ Å and $c=11.6416(1)$ Å at 80 K] and a (slightly) orthorhombic distorted [space group *Pmmm*, $a=3.86676(6)$ Å, $b=3.90145(4)$ Å, and $c=11.6742(1)$ Å at 80 K] one, as a consequence of clustering.[18] No diffraction peaks relative to impurity phases have been detected within any sample.

In order to study the diamagnetic contribution to the magnetization of the sample, we performed magnetization measurements with a MPMS-XL7 Quantum Design SQUID magnetometer, by using the RSO highly sensitive technique. The measurements have been performed in the temperature range 2–300 K at small constant magnetic field in zero-field-cooling (ZFC) and field-cooling (FC) conditions, and at different constant temperatures slightly above T_c by varying the

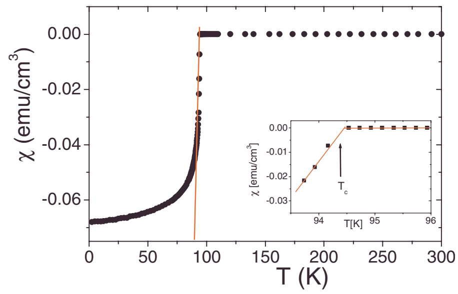

FIG. 1. (Color online) Diamagnetic susceptibility in $SmBa_2Cu_3O_7$ measured in powdered sample in magnetic field of 10 Oe. The solid line in the main figure gives an idea of the sharpness of the transition. In the inset the blow up of the data around the transition is reported, from which $T_c(H \approx 0) = 94.5 \pm 0.1$ K.

applied magnetic field after a ZFC process from room temperature.

III. EXPERIMENTAL RESULTS

Some experimental findings in optimally doped $SmBa_2Cu_3O_{\approx 7}$ are collected in Figs. 1–3. To extract the diamagnetic contribution to the magnetization, the measurements as a function of the field at 102 K, where the fluctuation contribution is no longer present, have been subtracted from the raw data. The sample is in powders while Eq. (2) in the text refers to the geometry of field along the c axis. On the other hand it has been shown[5] that for strong anisotropy factor γ the powder distribution is approximately equivalent to reduce the effective magnetization by a factor 1/3. The empty points correspond to magnetization measured after cooling at the same temperature in a given magnetic field (FC condition) and indicate that there are no history-dependent effects, as expected.

The sharpness of the transition, occurring at $T_c = 94.5 \pm 0.1$ K (a temperature slightly higher than in most of the YBCO-like compounds), is evidenced in Fig. 1. The transition temperature has been estimated by extrapolating the solid line of the main figure to the line of zero susceptibility, as usual in susceptibility measurements. Despite the procedure of measurements (field-cooling conditions, well known

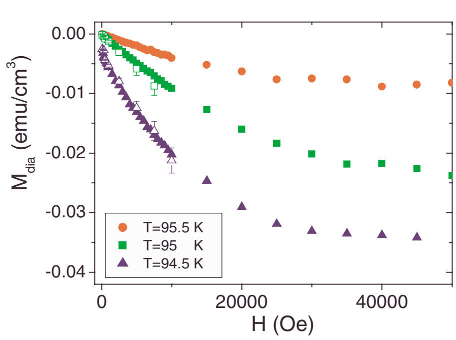

FIG. 2. (Color online) Isothermal magnetization curves M_{dia} vs H in the optimally doped $SmBa_2Cu_3O_{\approx 7}$ at three representative temperatures. The empty squares and triangles are the results obtained in FC condition (see text).

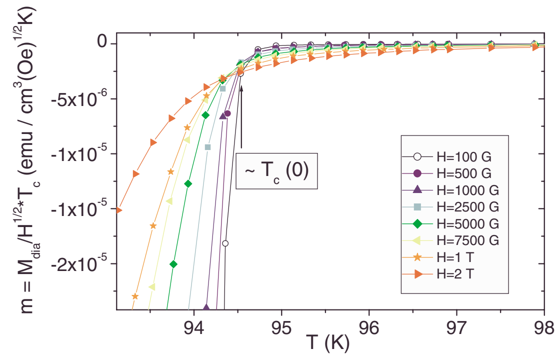

FIG. 3. (Color online) Scaled magnetizations $m = M_{dia}/T_c H^{1/2}$ as a function of temperature cross at about $T_c(0)$, consistently with the scaling arguments (Refs. 7 and 14) for anisotropic three-dimensional superconductors.

to broaden the transition), the transition is significantly sharp. Figure 2 shows how relatively far from T_c and for $H \ll H_{c2}$, M_{dia} is linear in H, while for $T \approx T_c$ one has $M_{dia} \propto H^{1/2}$ (Prange regime[1,2]). By increasing the field, saturation of SF-induced M_{dia} (Ref. 19) (provided that the contribution from short-wavelength fluctuations is still negligible) is somewhat displayed. The data for $M_{dia}/H^{1/2}$ (Fig. 3) as a function of temperature cross at $T_c(0)$, in agreement to scaling arguments,[9,23] as already discussed for optimally doped YBCO.[6,7,24–26] The reduced magnetization $m = M_{dia}/T_c H^{1/2}$ at $T_c(0)$ takes the value 2.3×10^{-6} emu/cm^3 Oe$^{1/2}$ K, consistent with the universal value $m_{3D}\gamma$ (Refs. 7, 23, and 25) for an anisotropy parameter γ around 6, close to the one in optimally doped YBCO.

Now we are going to illustrate how the scenario valid in optimally doped Sm-based cuprate has to be drastically modified in underdoped compounds. The susceptibility in the compound at $y = 0.15$ (namely, $SmBa_2Cu_{2.85}Al_{0.15}O_7$) (Fig. 4) indicates that the transition is less sharp than the one in the sample at $y = 0$, this being the obvious consequence of the Al for Cu substitution. The transition temperature for $H \to 0$ can be estimated $T_c = 56.5 \pm 0.5$ K, where the susceptibility turns out around 6.7×10^{-4} emu/cm^3, about a factor 30 larger than for $y = 0$. The magnetization vs temperature data at different magnetic fields H, at $T_c(0)$ do not scale as $M_{dia}/T_c H^{1/2}$ vs T (data not reported), thus giving a clear difference from

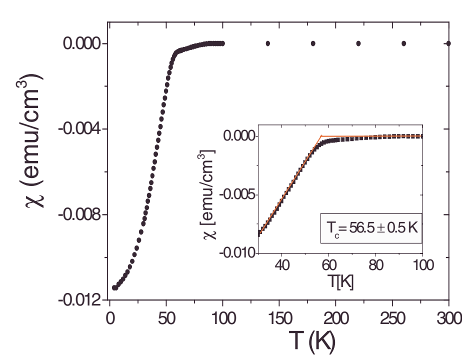

FIG. 4. (Color online) Diamagnetic susceptibility measured in the underdoped Sm-based superconductor at $y = 0.15$ in a field of 10 Oe. The sample is a reoxidized one (Ref. 12).

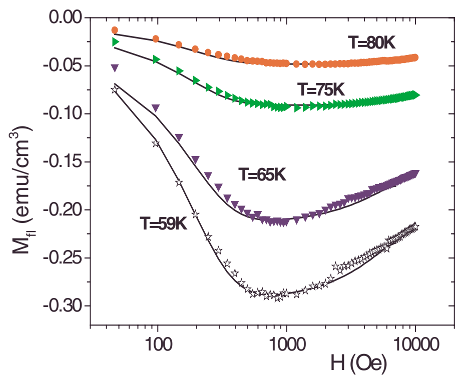

FIG. 5. (Color online) Representative isothermal magnetization curves M_{dia} vs H in the underdoped Sm-based superconductor at $y=0.15$ at $T_c(0)\approx 56.5$ K. The solid lines are the best fits according to the numerical integration of Eq. (4) in the text, in correspondence to the parameters reported in Table I.

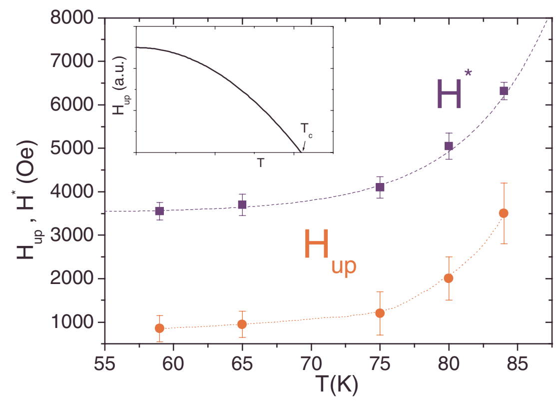

FIG. 6. (Color online) Upturn field H_{up} and characteristic field H^* (see text) as a function of temperature in $SmBa_2Cu_{2.85}Al_{0.15}O_7$ ($T_c=56.5$ K). The dotted line for H_{up} corresponds to the values obtained by setting $\chi(H)=0$ in Eq. (4) in the text and resorting to the interpolation of the best-fit parameters reported in Table I. The values of H^* (■), derived from the best fits of the magnetization curves, follow the almost linear relationship to H_{up}, according to Eqs. (4) and (5), for $T\leq 75$ K. The dashed line for H^* tracks the function $H^*(T)=[3520+3.5\times 10^{-3}\exp(T/6.2\text{ K})]$ Oe, heuristically found to describe rather well the data. The solid line in the inset represents a sketchy behavior of the upturn field in the case of diffuse transition. In the case of diffuse transition H_{up} mimics H_{c1} thus decreasing with T, contrary to what found by us in our underdoped compound.

optimally doped compound behavior. An even more striking difference with respect to the optimally doped compound appears in the magnetization curves (Fig. 5).

Compared to the curves in Fig. 2, in the data of Fig. 5 one notices the occurrence of an *extra diamagnetism*, with the peculiar characteristic of an upturn field in the range 500–2000 Oe. Evidently these magnetization curves cannot be justified on the basis of the conventional functional of the form in Eq. (2), which at variance leads to M_{dia} vs H consistent with the data in Fig. 2 for the optimally doped compound, as previously emphasized.

One might be tempted to justify the enhanced diamagnetism above T_c in underdoped cuprates as related to the occurrence of a diffuse transition. Because of chemical-type inhomogeneities (in a way a natural consequence of the Al for Cu substitution and of the annealing procedure) local transition temperatures $T_c^{loc}(\mathbf{r})$ above the bulk T_c might be suspected. Then for $T>T_c^{bulk}$ an enhanced diamagnetism would be detected, somewhat precursor of the Meissner effect for the bulk sample. In this case the upturn field would mimic H_{c1}, as due to the parts of the sample already in (nonpercolating) superconducting state. This hypothetical explanation does not apply to underdoped cuprates. In fact, if H_{up} in Fig. 5 should be the equivalent of H_{c1}, then it should decrease on increasing temperature. At variance, as displayed in Fig. 6 (main part), the upturn field increases on increasing temperature; as a contrast, in the inset the sketchy behavior of H_{up}, in the case it is led by diffuse transition due to chemical inhomogeneities, is reported. Consequently, we can conclude that the diamagnetic effects above T_c are not controlled by the chemical inhomogeneities. An increase in H_{up} with increasing temperature was already noticed in underdoped $La_{2-x}Sr_xCuO_4$ (LSCO).[27] However in that case the evidence about the temperature dependence of H_{up} was not so neat and Cabo *et al.*[28] could argue that it could still be compatible with a diffuse transition due to the inhomogeneities.

IV. ANALYSIS OF THE DATA IN THE UNDERDOPED COMPOUND

Now we are going to emphasize the unconventional character of the FD in the underdoped phases of cuprates by recalling the main lines of a theoretical description of the phenomenon. This theory helps in appreciating the data presented in the present report for Sm-based cuprates, meantime allowing one to emphasize relevant insights that can be achieved.[29]

The basic ingredient for unconventional FD in the underdoped, pseudogapped phases of superconductors is the marked dependence of the transition temperature on the carrier concentration. Then, above the transition temperature indicated by resistivity, one can argue that there are mesoscopic "islands" (corresponding to channels for the paraconductivity) with nonzero order parameter at frozen amplitude. The occurrence of long-range superconductivity is being prevented by the lack of coherence due to marked phase fluctuations. Experimental evidence of the existence of these islands at least in LSCO and in Bi-based cuprates, is provided by scanning SQUID microscopy[30] and by the detection of a large Nernst signal above T_c.[31]

Thus, by starting from Eq. (2), we keep $|\psi^2|$ constant and consider only the dependence on the phase, thus writing a Lawrence-Doniach-type (GLLD) functional of the form

$$F_{LD}[\theta]=\frac{1}{s}\sum_l\int d^2r \times\left\{J_{\parallel}\left(\nabla_{\parallel}\theta-\frac{2ie}{c\hbar}A_{\parallel}\right)^2+J_{\perp}[1-\cos(\theta_{l+1}-\theta_l)]\right\}, \tag{3}$$

where $J_{\parallel}$ and $J_{\perp}$ are the order-parameter phase coupling constants onto the plane and between planes, respectively.

TABLE I. Values of parameters used for M_{dia} vs H curves at different temperature $T(>T_c)$, from the fits by Eq. (4). H^* is the critical field reported in Eq. (4), L is the diameter of the mesoscopic islands above T_c, F the fraction of material at nonzero frozen order parameter, and $J_\parallel$ is the phase coupling constant in the plane.

T (K)	H^* (Oe)	L (nm)	F	Number of islands (cm^{-2})	$J_\parallel/k_BT$
59	3550	76.9	0.20	1.7×10^{12}	8.8
65	3700	75.3	0.16	1.5×10^{12}	3.9
75	4100	71.6	0.10	1.0×10^{12}	2.5
80	5050	64.5	0.06	8.7×10^{11}	0.8
84	6320	57.6	0.01	2.1×10^{11}	0.1

In this way one assumes the presence above the bulk T_c of superconducting "droplets" where the order-parameter phase can fluctuate producing thermal excitations (vortex and antivortex in two dimensions and vortex loops in the anisotropic model). The potential vector $A_\parallel$ in Eq. (3) describes both the magnetic field applied parallel to the c axis and the one induced by thermal fluctuations.

The second derivative of the free energy with respect to H (see Ref. 29 for more details) resulting from Eq. (3) yields the field-dependent susceptibility $\chi(H)$,

$$\chi = -\frac{k_BT}{s\Phi_0^2}\frac{1}{\langle 1+2n\rangle}\times\left\{\frac{\left[1+\left(\frac{H}{H^*}\right)^2\delta\right]^2}{n_{vor}}+s^2\gamma^2(1+n)n\left[1+\left(\frac{H}{H^*}\right)^2\delta\right]\right\} + 0.27L^2\frac{J_\parallel}{s}\left(\frac{2\pi}{\Phi_0}\right)^2\left(\frac{H}{H^*}\right)^2\delta \qquad (4)$$

with $\delta = J_\parallel/k_BT$, while $H^*=(\Phi_0/L^2)$ is a characteristic field, related to the size L of the islands (for all details about parameters and numerical factors we refer to Ref. 29). In Eq. (4) n is the number of planes at the interlayer distance s along which the vortex lines are correlated while γ is the anisotropy factor. The vortex density n_{vor} includes the vortices induced by the external field $n_H=(H/\Phi_0)$ as well as the thermally activated ones, whose density n_{th} is affected by the applied field, also depending from the number n of correlated layers,

$$n_{th} = n_0 \exp\left\{-\frac{E_0(1+2n)}{k_BT\left[1+\left(\frac{H}{H^*}\right)^2\delta\right]}\right\}. \qquad (5)$$

The prefactor in this equation can be set $n_0=6.6\times10^{18}$ cm^{-2} according to the relation $n_0\approx10^4/a^2$, for the lattice parameter $a=3.9$ Å. The third term in Eq. (4), being positive, is responsible of the inversion in the sign of the susceptibility and thus of the upturn in the magnetization curves.

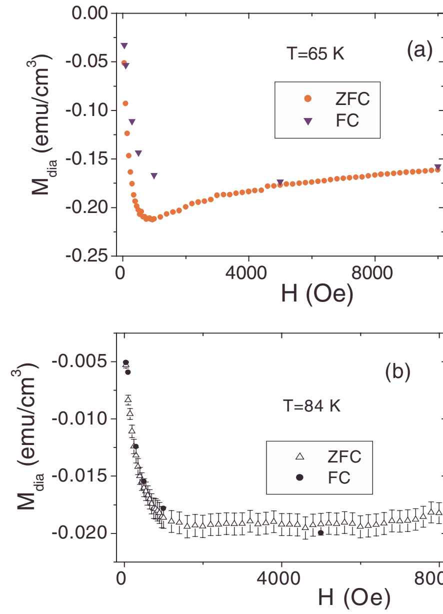

FIG. 7. (Color online) (a) Comparison of the magnetization data obtained in underdoped $SmBa_2Cu_{2.85}Al_{0.15}O_7$ in the usual zero-field-cooling condition with the values (triangles) of the magnetization measured after cooling the sample at the same temperature in presence of an applied magnetic field (field-cooling condition). (b) Comparison of ZFC and FC magnetization measurements carried out at a temperature expected well above an average local irreversibility temperature. At variance with the data in (a), FC and ZFC M_{dia} coincide and the region of positive $\chi(H)$ is practically absent.

By means of numerical integration of Eq. (4) the isothermal diamagnetic magnetization as a function of the field is obtained. In Fig. 5 the solid lines M_{dia} vs H derived in this way are the best fits of the experimental data, in correspondence to the parameters collected in Table I.

The interlayer distance has been set $s=11.7$ Å according to the structural data from x-ray diffraction[18] while the anisotropy factor was taken $\gamma=6$, according to the experimental findings (Fig. 3). According to our fitting the quantity $E_0(1+2n)=86k_BT_c$ turns out almost temperature independent. This corresponds to the deduction that the number of correlated layers does not change in a sizeable way in the temperature range that has been explored. Furthermore, the activation energy in Eq. (5) turns out $E_0\approx12k_BT_c$ (for $n=3$) in accordance to the general estimate in YBCO of E_0 around $10k_BT_c$.[8,29]

From the characteristic field H^* it is possible to estimate an order of magnitude of the average size L of the islands (Table I). As it could be expected, on increasing temperature, the areas with nonzero order parameter are progressively reduced in size. A reduction factor F accounting for the fraction of the whole volume of the sample which contributes to the diamagnetic response can be derived. The values of the fraction F (Table I), as it could be expected, indicate a progressive decrease in the volume occupied by the superconducting regions. It should be remarked that the reduction in the effective volume may be due both to the decrease in the average size of the islands and/or to the decrease in their number, that could be evaluated from the ratio $V_S F/L^3$, $V_S=3.9\times10^{-3}$ cm^3 being the volume of the sample.

Finally we remark that a significant phenomenon that might be present involves history-dependent effects, i.e., *irreversibility*. The islands where the amplitude of the order parameter is frozen can be above or below their irreversibility temperature T_{irr}. If a measure is carried out at $T<T_{irr}$ then history-dependent effects should be present. In Fig. 7 the comparison of the usual ZFC magnetization curve with the values of M_{dia} measured at the same temperature after cooling in the presence of a given applied field (field cooling, FC), is reported.

In our interpretative model the irreversibility line has to be attributed to vortex-loop unbinding and to the generation of a liquid of vortices. Therefore T_{irr} corresponds to the Kosterlitz-Thouless transition temperature (T_K). The behaviors for temperatures above or below T_K is controlled by the ratio $J_{\parallel}/k_B T$, which is larger than 2 at $T<T_K$ while it drops to zero above the irreversibility line, where a marked upturn in the magnetization curves is not expected.

According to theory sketched above, the history-dependent effects have to disappear when the measuring temperature is brought above the local T_{irr}. Meantime the upturn in the field dependence of M_{dia}, namely, *positive susceptibility* [Eq. (4)] has to be modified, M_{dia} becoming practically flat in the high field range. This effect has been detected as well [Fig. 7(b)].

V. SUMMARIZING REMARKS

By taking advantage of the excellent superconducting properties of Sm-based cuprates, a detailed study of the fluctuating diamagnetism above T_c has been carried out. In the optimally doped compound the conventional GL scenario of the superconducting fluctuations has been confirmed. At variance, in the underdoped compound, where the pseudogapped phase is known to be present, the experimental data show dramatic departure from that theoretical framework, with strong enhancement of the susceptibility and isothermal magnetization curves exhibiting an upturn in the field dependence. The temperature dependence of the upturn field rules out the hypothesis of a possible diffuse transition. On the contrary, several experimental data support a theoretical picture of unconventional fluctuating diamagnetism based on the idea of precursor islands where the amplitude of the order parameter is frozen, while the long-range coherence granting a bulk superconducting state is prevented by marked fluctuations in the phase of the order parameter. It is argued that this phenomenon is characteristic of the pseudogap phase of the superconducting cuprates.

[1] A. I. Larkin and A. A. Varlamov, *Theory of Fluctuations in Superconductors* (Oxford University Press, New York, 2005).

[2] M. Tinkham, *Introduction to Superconductivity* (McGraw-Hill, New York, 1996), Chap. 8.

[3] J. Kurkijarvi, V. Ambegaokar, and G. Eilenberg, Phys. Rev. B **5**, 868 (1972).

[4] A. I. Larkin and A. A. Varlamov, *Theory of Fluctuations in Superconductors* (Ref. 1), Sec. 2.3.1.

[5] For application of the zero-dimensional condition to fluctuating diamagnetism, see A. Lascialfari, T. Mishonov, A. Rigamonti, P. Tedesco, and A. A. Varlamov, Phys. Rev. B **65**, 180501(R) (2002); and E. Bernardi, A. Lascialfari, A. Rigamonti, L. Romanò, V. Iannotti, G. Ausanio, and C. Luponio, *ibid.* **74**, 134509 (2006).

[6] C. Baraduc, A. Buzdin, J. Y. Henry, J. P. Brison, and L. Puech, Physica C **248**, 138 (1995).

[7] A. Junod, J.-Y. Genoud, G. Triscone, and T. Schneider, Physica C **294**, 115 (1998).

[8] A. Lascialfari, A. Rigamonti, L. Romanò, P. Tedesco, A. Varlamov, and D. Embriaco, Phys. Rev. B **65**, 144523 (2002).

[9] See Fig. 2.3 in Ref. 1.

[10] M. R. Norman, D. Pines, and C. Kallin, Adv. Phys. **54**, 715 (2005).

[11] P. A. Lee, Rep. Prog. Phys. **71**, 012501 (2008).

[12] N. H. Andersen, M. von Zimmermann, T. Frello, M. Käll, D. Mønster, P.-A. Lindgård, J. Madsen, T. Niemöller, H. F. Poulsen, O. Schmidt, J. R. Schneider, Th. Wolf, P. Dosanjh, R. Liang, and W. N. Hardy, Physica C **317-318**, 259 (1999); P. G. Radaelli, in *Neutron Scattering in Layered Copper-Oxide Superconductors*, edited by A. Furrer (Kluwer Academic, Dordrecht, Boston, London, 1998), pp. 23–83, and references therein.

[13] M. v. Zimmermann, J. R. Schneider, T. Frello, N. H. Andersen, J. Madsen, M. Käll, H. F. Poulsen, R. Liang, P. Dosanjh, and W. N. Hardy, Phys. Rev. B **68**, 104515 (2003).

[14] J. Strempfer, I. Zegkinoglou, U. Rütt, M. v. Zimmermann, C. Bernhard, C. T. Lin, Th. Wolf, and B. Keimer, Phys. Rev. Lett. **93**, 157007 (2004).

[15] M. Scavini, L. Mollica, and L. Malavasi, Solid State Sci. **6**, 1187 (2004).

[16] M. Scavini and R. Bianchi, J. Solid State Chem. **161**, 396 (2001).

[17] E. Brecht, W. W. Schmahl, G. Miehe, M. Rodewald, H. Fuess, N. H. Andersen, J. Hanßmann, and Th. Wolf, Physica C **265**, 53 (1996).

[18] M. Scavini, M. Daldosso, S. Cappelli, C. Oliva, M. Brunelli, C. Ferrero, and A. Lascialfari, Europhys. Lett. **76**, 443 (2006).

[19] A. E. Koshelev, Phys. Rev. B **50**, 506 (1994).

[20] A. N. J. Fitch, J. Res. Natl. Inst. Stand. Technol. **109**, 133 (2004).

[21] A. C. Larson and R. B. Von Dreele, Los Alamos National Laboratory Report No. LAUR 86–748, 2004 (unpublished).

[22] B. H. Toby, J. Appl. Crystallogr. **34**, 210 (2001).

[23] T. Schneider and J. M. Singer, *Phase Transition Approach to High Temperature Superconductivity* (Imperial College, London, 2000), Chap. 6.

[24] M. A. Hubbard, M. B. Salamon, and B. W. Veal, Physica C **259**, 309 (1996).

[25] T. Mishonov and E. Penev, Int. J. Mod. Phys. B **14**, 3831 (2000).

[26] V. G. Kogan, M. Ledvij, A. Yu. Simonov, J. H. Cho, and D. C. Johnston, Phys. Rev. Lett. **70**, 1870 (1993).

[27] A. Lascialfari, A. Rigamonti, L. Romanò, A. A. Varlamov, and I. Zucca, Phys. Rev. B **68**, 100505(R) (2003).

[28] L. Cabo, F. Soto, M. Ruibal, J. Mosqueira, and F. Vidal, Phys. Rev. B **73**, 184520 (2006).

[29] This theoretical picture follows from the inspiring idea of A. Sewer and H. Beck, Phys. Rev. B **64**, 014510 (2001), introduced at the aim of justifying early magnetization curves detected in underdoped YBCO; [P. Carretta, A. Lascialfari, A. Rigamonti, A. Rosso, and A. A. Varlamov, *ibid.* **61**, 12420 (2000)]; Significant steps in the theory were introduced in the paper in Ref. 8. For a comprehensive illustration of the basic aspects of the theory, see L. Romanò, Int. J. Mod. Phys. B **17**, 423 (2003), and Ref. 8.

[30] I. Iguchi, T. Yamaguchi, and A. Sagimoto, Nature (London) **412**, 420 (2001).

[31] Y. Wang, L. Li, and N. P. Ong, Phys. Rev. B **73**, 024510 (2006).